COMPREHENSIVE ANALYSIS OF DAMAGE PROGRESSION IN HIGH-PERFORMANCE THERMOPLASTIC COMPOSITES THROUGH MULTI-INSTRUMENTAL STRUCTURAL HEALTH MONITORING APPROACHES

Ceren Yildirim[1,2], Isa Emami Tabrizi [3], Abdulrahman Al-Nadhari [1,2], Serra Topal [1,2] , Bertan Beylergil [4] Mehmet Yildiz [1,2]

[1] Sabanci University Integrated Manufacturing Technologies Research and Application Center & Composite Technologies Center of Excellence, Teknopark Istanbul, Pendik, Istanbul 34906, Turkey
[2] Faculty of Engineering and Natural Sciences, Sabanci University, Tuzla, Istanbul 34956, Turkey
[3] College of Science and Engineering, University of Derby, Kedleston Rd, Derby, DE22 1GB, UK
[4] Faculty of Engineering, Department of Mechanical Engineering, Alanya Alaaddin Keykubat University, 07450, Alanya, Turkey

Presenting author. *yildirimceren@sabanciuniv.edu*

Keywords: Thermoplastic composites; Automated fiber placement (AFP); Damage characterization; Digital Image Correlation; Acoustic Emission; Thermography

Abstract

The failure behavior of carbon fiber/poly(ether ketone ketone) (CF/PEKK) composites manufactured via automated fiber placement (AFP) followed by subsequent consolidation in autoclave is studied. Multi-instrumental structural health monitoring (SHM) approaches are used to analyze damage development stages and and damage types in high performance thermoplastic composite laminates. Void analysis, and density measurement, and optical microscopy reveal the effect of secondary consolidation through autoclave on the microstructure of the composite laminates. An interlaminar void reduction from 5.65% to 0.46% are observed. Acoustic emission (AE), digital image correlation (DIC), and infrared thermography (IRT) techniques during tensile tests provide complementary understanding of the physics behind the critical damage types occurring in the material, such as edge splitting. Slope of the cumulative AE counts and percentage of total number of hits signify two distinct stages of failure, each associated with a dominant failure mode. Also it is evident that the high energy AE hits are corresponding to macro level damage events which are captured by the IRT in the form of various edge splitting. The initiation of these damage events can be anticipated through concurrent monitoring of DIC strain maps.

1. Introduction

High-performance thermoplastic matrix composites (TPCs) are increasingly favored for aerospace applications due to a multitude of advantages, such as notable strength-to-weight ratios, expedited molding processes, exceptional resistance to environmental factors, recyclability, and the capability for room temperature storage [1,2]. Within the realm of TPCs, Polyetherketoneketone (PEKK) stands out for its remarkable structural advantages, characterized by high mechanical toughness, favorable formability, low moisture absorption, and strong bonding properties [3,4].

Understanding damage onset and evaluation in composites is crucial for ensuring structural integrity and facilitating safer design practices. There is a growing need for alternative and complementary monitoring methods to investigate damage accumulation in composite materials [5,6]. This research integrates a comprehensive structural health monitoring system with mechanical testing to analyze the characterization of damage mechanisms, including their development and classification, in high-performance thermoplastic composites (TPCs) produced through Automated Fiber Placement (AFP) technology, specifically those composed of Carbon Fiber/Polyetherketoneketone (CF/PEKK).

2. Materials and Methods

Three unidirectional laminates are produced using a robotic laser-assisted Automated Fiber Placement (AFP) system (Coriolis C1), with a feed rate of 0.2 m/s and a consolidation force of 400 N (see in **Figure 1a**). The visible nip-point temperature is recorded at 400±10 °C. After the lay-up process, the laminate is cooled down to room temperature and removed. Consolidation of the AFP CF/PEKK thermoplastic lay-up occurs in an autoclave environment using the ASC autoclave system, with a consolidation temperature of 377 °C, heating, and cooling ramps of 5 °C/min and 11 °C/min, and a pressure of 8 bars maintained constant for 40 minutes (see in **Figure 1b**).

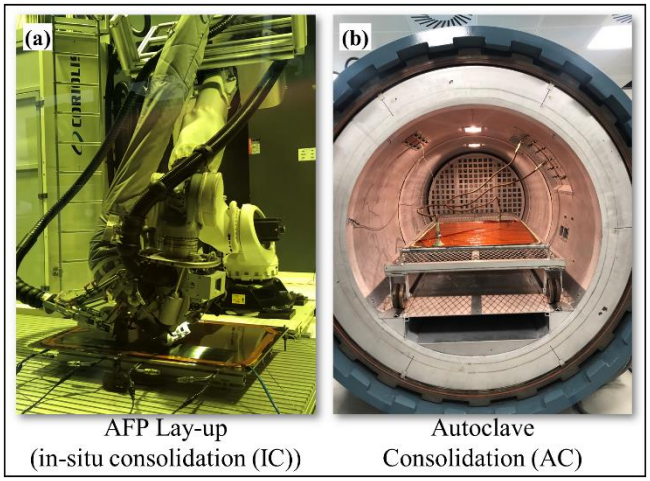

Figure 1. CF/PEKK Composite Manufacturing

To obtain the void content of in-situ and autoclave consolidated CF/PEKK laminates, fiber, matrix, and void contents of these specimens are measured based on the ASTM D3171 standard method 1. Also, the effect of secondary consolidation on the microstructure of the composite is thoroughly investigated using a Nikon, ECLIPSE LV100ND model microscopy.

2.1. Multi-instrument Structural Health Monitoring Techniques

Tensile tests are conducted on CF/PEKK composite specimens at a speed of 1.5 mm/min using an INSTRON 5982 universal testing machine. A bi-axial strain gauge is affixed to the specimen surface to measure the Poisson ratio. Throughout the tests, specimens are monitored using multi-instrument structural health monitoring techniques, including AE, DIC, and passive IRT, as depicted in **Figure 2**.

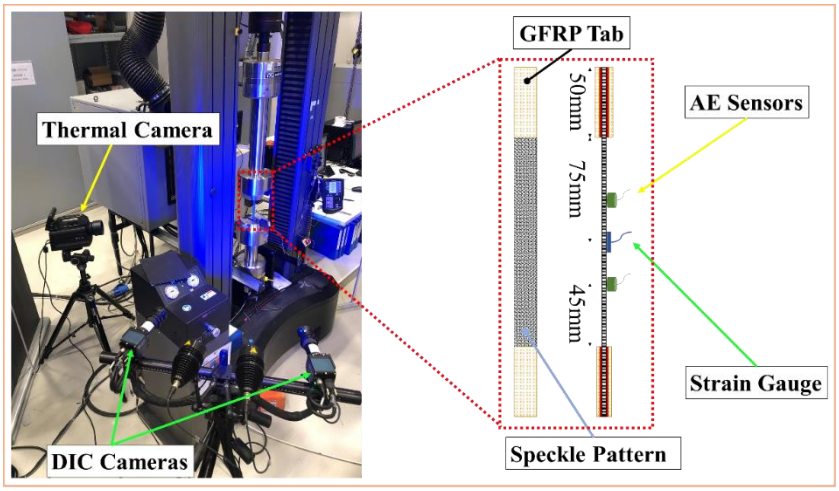

Figure 2. Multi-instrument Structural Health Monitoring.

3. Results

3.1. Impact of secondary consolidation on the microstructure of the composite

The average densities of three samples from in-situ and autoclave consolidated CF/PEKK composite plates are 1.49 and 1.58 g/cm3, respectively. **Table 1** presents the corresponding average weight fractions of fiber (W_f) and matrix (W_m), along with the volume percent contents of fiber (V_f), matrix (V_m), and void (V_v) for both consolidation methods.

Table 1 Fiber, matrix, and void contents of in-situ and autoclave-consolidated laminates.

	W_f (%)	**W_m (%)**	**V_f (%)**	**V_m (%)**	**V_v (%)**
In-situ consolidated (IC) CF/PEKK	65.04 ± 0.26	34.96 ± 0.26	54.22 ± 0.20	40.13 ± 0.31	5.65 ± 0.13
Autoclave-consolidated (AC) CF/PEKK	65.29 ± 0.14	34.71 ± 0.14	57.47 ± 0.16	42.07 ± 0.15	0.46 ± 0.04

As seen in **Table 1** the void content of autoclave consolidated CF/PEKK composite is less than 1%, i.e. minimum acceptable range in high performance composite laminates. As seen in **Figure 3** the large portion of voids in the microstructure of in-situ consolidated composites are pseudo-interconnected interlaminar voids at intimate contact lines. Autoclave processing not only helps to reduce the size of voids but also provides a network of pathways for removal of trapped air via bleeding. As a result, the void content decreases from 5.65% to 0.46%.

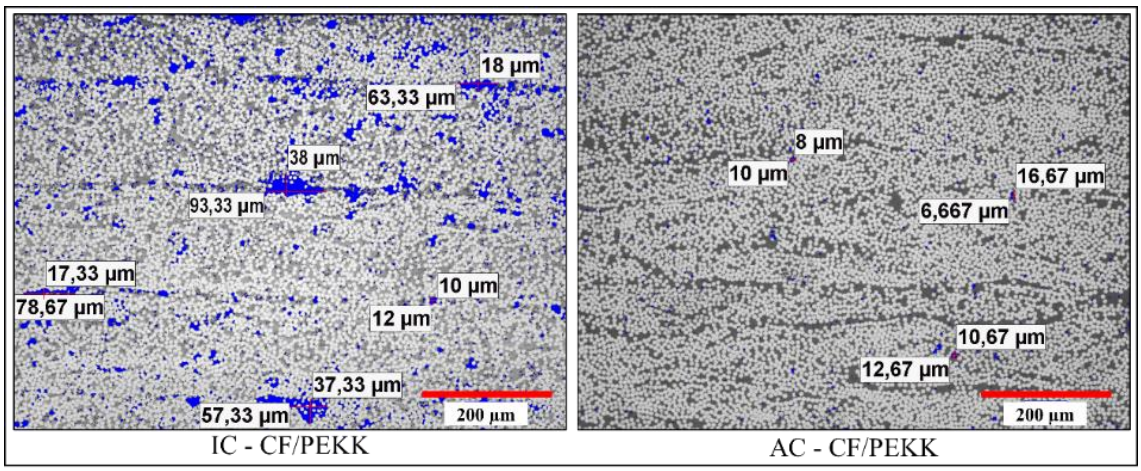

Figure 3. Optical microscope images of in-situ and autoclave consolidated laminate.

3.2. Multi-instrument Nondestructive Monitoring

The identified types of failure have been categorized based on their Weighted Peak Frequency (WPF) [7–9], spanning from low to high, as outlined in **Table 2**. The representative clustering of AE hits tensile samples of CF/PEKK is given in **Figure 4a.** Partial Power 2 indicates to the percentage of signal power in the frequency range of 300–600 kHz. WPF is calculated using Equation (1) as:

$$WPF = (f_c \times f_p)^{1/2} \quad (1)$$

where f_c and f_p indicate the frequency centroidand peak frequency, respectively.

Table 2 WPF range and related failure type.

WPF Range (kHz)	Failure Type
50-190	Matrix Cracking (MC)
190-360	Interface Failure (IF)
360-550	Fiber Failure (FF)

In **Figure 4b**, the amplitude of AE hits and the cumulative AE counts versus time graphs for CF/PEKK composite specimens are depicted. Notably, the cumulative AE count curve reveals two distinct stages called as stage I and stage II, respectively. In the region designated as Stage I, the AE counts demonstrate a linear increase, suggesting a consistent progression of damage within the laminate. In this stage, the AE hits associated with matrix cracking and interface failure exhibit both high and low amplitudes. Contrary to Stage I, Stage II displays a non-linear rise in cumulative AE counts over time, predominantly consisting of low-amplitude AE events. Notably, the frequent incidence of high-amplitude interface failures, such as delamination events observed in Stage I, is absent in Stage II. Although low- and high-amplitude delamination failures are evident in thermoplastic laminates, their occurrence frequency varies depending on the severity of accumulated damage within the material. **Figure 4c** illustrates the percentage of failure in these two stages, indicating a transition from matrix failure to fiber failure.

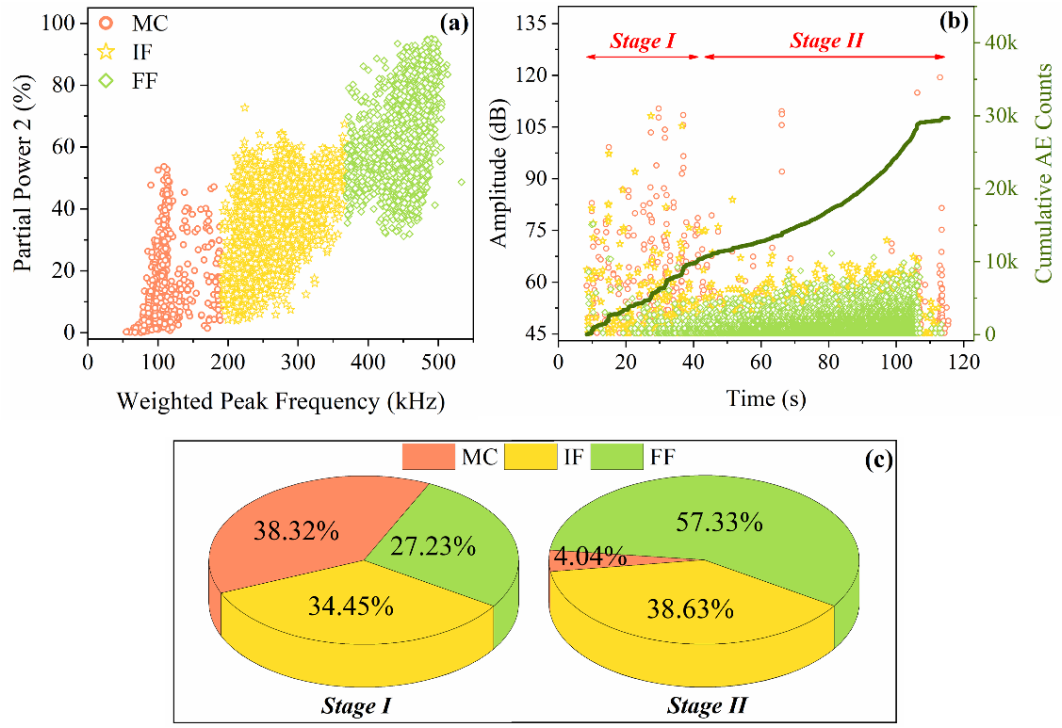

Figure 4. (a) Representative k-means clusters for tensile samples and **(b)** variations of time versus amplitude and cumulative AE counts, and **(c)** number of hits for various damage types

Figure 5 presents the plot of cumulative AE energy and load versus time. The fact that the axial strains-over time obtained from SG and DIC are the same with each other, which means that the DIC method is reliable for this study. Also, there is a deviation between axial strain curves and load curve at the end of the Stage I. At this stage, fiber-dominant failures control the material fracture, concomitant with a reduction in slope observed in the strain-time curve, indicative of an augmented stiffness in the laminates. There are five significant changes in the load versus time curve, marked as i, ii, iii, iv and v. All points (i-v) are also detected by AE, SG, DIC and IRT system, however, after point ii, AE sensor failed to record data.

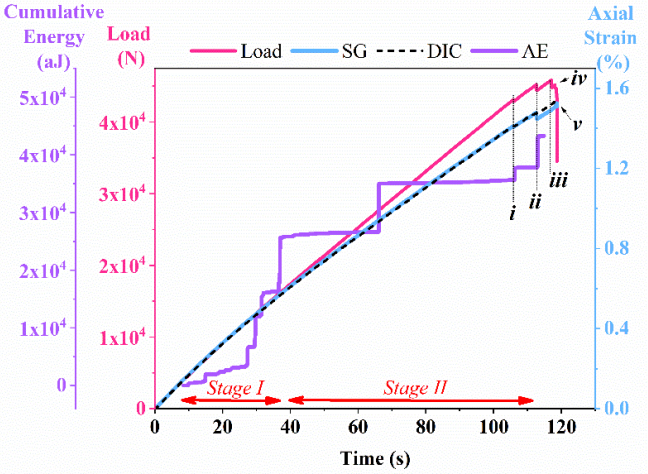

Figure 5. Plots of total AE cumulative energy, load, and axial strain over time. Note: Points (i), (ii), (iii), (iv), and (v) are marked to show the activity at 106, 113, 117, 118 and 119 s, respectively.

Thermal maps and strain maps corresponding to the time intervals (i-v) are depicted in **Figure 6**. Edge splitting, attributed to fiber misalignment at the edges of the composite specimen, is clearly observed from the beginning to the final stages of the tensile test in the IRT maps. Additionally, as depicted in the DIC map, localized high strain regions encircled in the specimen's edges are more pronounced. This suggests that the edge regions of the specimen are more susceptible to damage initiation and growth. Despite the expectation of greater deformation and earlier failure in regions with higher strain regions, it is noteworthy that the top left side of the specimen fails at an early stage, while the lower left region remains unaffected. The comparison between DIC strain maps and corresponding thermal maps indicates that the high strain gradient region at the lower left edge of the sample emerges at 67% of the maximum stress, while thermography maps do not exhibit any relevant activity in the same region until 90% of the ultimate tensile strength is reached. This observation underscores the capability of DIC results to identify failure-prone areas in TPCs well in advance compared to other techniques.

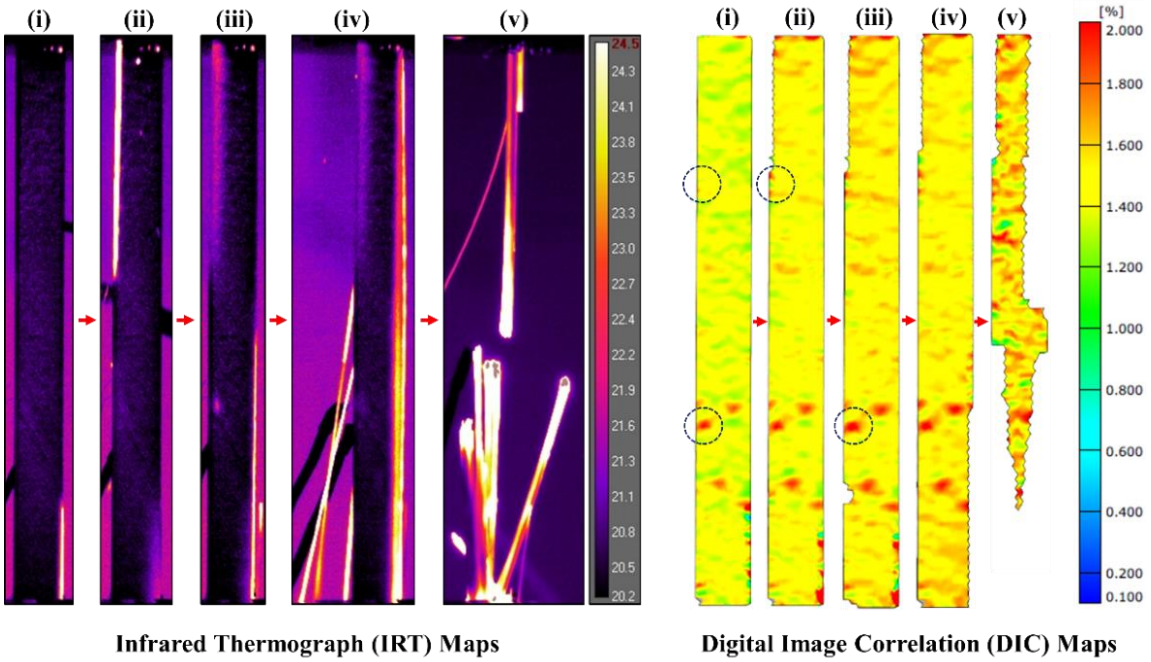

Figure 6. Thermograms and DIC in-plain strain fields for CF/PEKK specimens at (i) 106, (ii) 113, (iii) 117, (iv) 118, and (v) 119 s corresponding to the points marked in **Figure 5.**

4. Conclusions

This study investigates the impact of autoclave consolidation following in-situ consolidation on the microstructural properties of unidirectional CF/PEKK TPCs and examines damage mechanisms under tensile loading using multi-instrumental monitoring techniques. Microscopic observations reveal a reduction in voids within in-situ consolidated laminates post-autoclave consolidation, enhancing material intimacy. Analysis of AE hits and counts demonstrates a shift in tensile failure behavior from matrix-dominant to fiber-dominant failure modes, coinciding with a gradual stiffness increase. This change in AE hits may serve as a damage index in thermoplastic laminates, aiding in assessing composite structure longevity. Correlation between AE energy upsurges and macro-level damage detected by thermal imaging links to edge splitting, predictable through DIC strain maps. However, DIC maps provide insufficient data on the likelihood of these macro damage events due to the stochastic nature of fiber failures in carbon fiber-reinforced laminates. Furthermore, DIC allows susceptible failure areas in thermoplastic materials to be identified much earlier than IRT methodologies.

Acknowledgments
The authors gratefully acknowledge financial support from the Scientific and Technological Research Council of Turkey (TÜB˙ITAK) with project number 218M709. C. Yildirim gratefully acknowledges the financial support provided by the European Cooperation in Science & Technology (COST) under Action CA21155 to her attendance at the 21st European Conference on Composite Materials (ECCM21).

References

[1] Hoang VT, Kwon BS, Sung JW, Choe HS, Oh SW, Lee SM, et al. Postprocessing method-induced mechanical properties of carbon fiber-reinforced thermoplastic composites. J Thermoplast Compos Mater 2023;36:432–47. https://doi.org/10.1177/0892705720945376.

[2] Sudhin AU, Remanan M, Ajeesh G, Jayanarayanan K. Comparison of Properties of Carbon Fiber Reinforced Thermoplastic and Thermosetting Composites for Aerospace Applications. Mater. Today Proc., vol. 24, Elsevier; 2020, p. 453–62. https://doi.org/10.1016/j.matpr.2020.04.297.

[3] Yildirim C, Ulus H, Beylergil B, Al-Nadhari A, Topal S, Yildiz M. Tailoring adherend surfaces for enhanced bonding in CF/PEKK composites: Comparative analysis of atmospheric plasma activation and conventional treatments. Compos Part A Appl Sci Manuf 2024:108101. https://doi.org/10.1016/J.COMPOSITESA.2024.108101.

[4] Yildirim C, Ulus H, Beylergil B, Al-Nadhari A, Topal S, Yildiz M. Effect of atmospheric plasma treatment on Mode-I and Mode-II fracture toughness properties of adhesively bonded carbon fiber/PEKK composite joints. Eng Fract Mech 2023;289:109463. https://doi.org/https://doi.org/10.1016/j.engfracmech.2023.109463.

[5] Saeedifar M, Zarouchas D. Damage characterization of laminated composites using acoustic emission: A review. Compos Part B Eng 2020;195:108039. https://doi.org/10.1016/j.compositesb.2020.108039.

[6] Ivanov SG, Beyens D, Gorbatikh L, Lomov S V. Damage development in woven carbon fibre thermoplastic laminates with PPS and PEEK matrices: A comparative study. J Compos Mater 2017;51:637–47. https://doi.org/10.1177/0021998316653460.

[7] Ali HQ, Emami Tabrizi I, Khan RMA, Tufani A, Yildiz M. Microscopic analysis of failure in woven carbon fabric laminates coupled with digital image correlation and acoustic emission. Compos Struct 2019;230. https://doi.org/10.1016/j.compstruct.2019.111515.

[8] Tabrizi IE, Kefal A, Zanjani JSM, Akalin C, Yildiz M. Experimental and numerical investigation on fracture behavior of glass/carbon fiber hybrid composites using acoustic emission method and refined zigzag theory. Compos Struct 2019;223:110971. https://doi.org/10.1016/j.compstruct.2019.110971.

[9] Yildirim C, Tabrizi IE, Al-Nadhari A, Topal S, Beylergil B, Yildiz M. Characterizing damage evolution of CF/PEKK composites under tensile loading through multi-instrument structural health monitoring techniques. Compos Part A Appl Sci Manuf 2023;175:107817.

https://doi.org/https://doi.org/10.1016/j.compositesa.2023.107817.